View Online / Journal Homepage / Table of Contents for this issue
Dynamic Article Links

Analyst

Cite this: *Analyst*, 2011, **136**, 5234

www.rsc.org/analyst

**PAPER**

# Development and evaluation of a highly sensitive rapid response enzymatic nanointerfaced biosensor for detection of putrescine

**Saranya Shanmugam,[a] Kavitha Thandavan,[a] Sakthivel Gandhi,[a] Swaminathan Sethuraman,[a] John Bosco Balaguru Rayappan[b] and Uma Maheswari Krishnan*[a]**

***Received 23rd July 2011, Accepted 21st September 2011***
**DOI: 10.1039/c1an15637c**

Published on 21 October 2011 on http://pubs.rsc.org | doi:10.1039/C1AN15637C
Downloaded by University of Guelph on 07 September 2012

Putrescine (1,4-diaminobutane) a biologically active diamine has been found to be a valuable analyte for several clinical and analytical purposes. The present work deals with diamine oxidase immobilized on iron oxide nanoparticles for quantifying the amount of putrescine produced, by the decarboxylation of ornithine, which is converted into hydrogen peroxide by the enzyme diamine oxidase (DAO). This reaction can be quantified using electrochemical techniques, which forms the basis of this work. Iron oxide ($Fe_3O_4$) nanoparticles, synthesized using thermal co-precipitation, were chosen for immobilization of DAO due to its simple preparation procedure, high surface area and cost-effectiveness. The size of the particles was in the range of 25–35 nm and the enzyme was linked covalently by carbodiimide activation and confirmed using FT-IR. For detecting the hydrogen peroxide released in the reaction, a glassy carbon-working electrode coated with enzyme linked iron oxide nanoparticles was poised at +0.4 V *versus* an Ag/AgCl reference electrode and a platinum wire was used as the counter electrode. A step-wise increase in current was observed and linearity was obtained in the range of 2–8 nM, with 0.65 nM as the minimum detection limit and the response time was found to be 0.3 seconds. Ascorbic acid, a common interfering molecule in biological samples, did not interfere with the measurements indicating the high degree of specificity of the diamine oxidase-based nano-interfaced biosensor.

## 1. Introduction

Polyamines such as putrescine, spermidine and spermine are biologically active amines, which are essential for many cellular processes such as cell growth, cell proliferation and cell differentiation in cells that are both malignant and normal.[1] Among them, putrescine has been implicated for the foul odour of putrefying flesh, bad breath and bacterial vaginosis. Abnormally high levels of putrescine have been associated with Menky's Kinky hair disease, a heritable copper deficiency disorder.[2] Putrescine, when present at high concentrations in the mammalian brain, has an influence in modulating depression. Putrescine levels in plasma of the renal failure patients have been shown to be elevated.[3] Since putrescine plays a very important role in the metabolism of various biological tissues, its detection even at very low concentrations is critical. It was found that most of the polyamines circulating in blood are localized in the erythrocytes, their content in normal human blood being spermidine 14.1 ± 3.1, and spermine 8.4 ± 2.8 nmol $mL^{-1}$ packed erythrocytes. Putrescine is not present in normal human erythrocytes. The polyamine level in serum is less than 0.1 nmol $mL^{-1}$. The polyamine content of the erythrocytes from patients with malignant neoplasm was significantly elevated.[4]

The basic principle in the detection of putrescine is its conversion to hydrogen peroxide by diamine oxidase. Diamine oxidase (E.C: 1.4.3.6) also known as histaminases is a copper-containing enzyme found in human intestinal mucosa.[5]

$$\text{Putrescine} + H_2O + O_2 \xrightarrow{\text{DAO}} H_2O_2 + \text{4-Aminobutanal} + NH_3$$

Conventional HPLC techniques have been employed to determine the levels of biogenic amines.[6] Previously an amperometric diamine sensor was developed for clinical applications in the diagnosis of bacterial vaginosis based on putrescine oxidase (crosslinked), which catalysed the conversion of diamines to products including hydrogen peroxide. This sensor demonstrated a linear dynamic range from 0.5–300 μM for putrescine and a response time of 20 s.[7] L. Nagy *et al.* developed an amperometric biosensor for the *in vitro* measurement of low concentration of putrescine in blood, which had a detection

[a]*Centre for Nanotechnology & Advanced Biomaterials, School of Chemical & Biotechnology, SASTRA University, Thanjavur, 613 401, India. E-mail: umakrishnan@sastra.edu; Fax: +91 4362 264120; Tel: +91 4362 304000 ext: 677*
[b]*Centre for Nanotechnology & Advanced Biomaterials, School of Electrical & Electronics Engineering, SASTRA University, Thanjavur, 613 401, India*


This journal is © The Royal Society of Chemistry 2011

Published on 21 October 2011 on http://pubs.rsc.org | doi:10.1039/C1AN15637C
Downloaded by University of Guelph on 07 September 2012

limit of 50 nM.[8] Similarly another amperometric biosensor for detection of diamine using diamine oxidase purified from porcine kidney and a platinum working electrode was linear up to 6 mM histamine, cadaverine, or putrescine with a lower detection limit of 25 μM.[9] A hydrogen peroxide biosensor based on peroxidase activity of haemoglobin in a polymeric film with linear detection range from 5 to 125 μM has been developed.[10] An amino oxidase amperometric biosensor for polyamines in which the linear calibration range is 0.5–10 μM of putrescine, with a lower detection limit of 0.2 μM and the response time of 15 to 60 s.[11] An enzyme sensor array for the determination of biogenic amines in food samples has a lowest detection limit of 5 mg $kg^{-1}$ putrescine.[12]

Use of a nanointerface for sensing applications has gained popularity due to better sensitivity, improved response time, enhanced electron transfer rates and minimal analyte volume.[13,14] In the recent years, Shen *et al.*[15] reported the direct electrochemistry of haemoglobin on carbonized titania nanotubes and its application in a sensitive reagentless hydrogen peroxide biosensor. The developed sensor offered a low detection limit of 0.92 μM and a quick response time of 3 s. It offered a high dynamic response range of $10^{-6}$ to $10^{-4}$ M with a heterogeneous electron transfer rate constant (kET) 108 $s^{-1}$.

Guo *et al.*[16] reported the biointerface by cell growth on layered graphene–artificial peroxidase–protein nanostructure for *in situ* quantitative molecular detection. The developed sensor showed a fast response time of 5 s, with a wide linear detection range up to $100 \times 10^{-6}$ M. A high sensitivity of 4.5 μA $\mu M^{-1}$ $cm^{-2}$ and a low detection limit of $0.1 \times 10^{-6}$ M ($S/N = 3$) was reported. The same group reported thin-walled graphitic nanocages as a unique platform for amperometric glucose biosensor. The linear response range, detection limit, sensitivity and response time are found to be 0.02 to 6.2 mM, 8 μM, 13.3 μA $mM^{-1}$ $cm^{-2}$, <5 seconds respectively.[17] Recently, Guo *et al.*[18] reported a unique HRP/Au NPs/PANI nanofibre biofilm for the *in situ* molecular detection of ischemic cells in which a fast response of 3 seconds, high sensitivity of 117.8 mA $mM^{-1}$ $cm^{-2}$, with a low detection limit of 0.3 μM and the electron transfer rate constant of 3.52 $s^{-1}$ were obtained.

Recently, iron oxide nanoparticles have been used in biosensors for detecting biogenic compounds. Iron oxide nanoparticles–chitosan composite based glucose biosensor was developed with a linear detection range of 10–400 mg $dL^{-1}$.[19] Iron oxide nanoparticles–multiwalled carbon nanotubes matrix was used to immobilize acetylcholine esterase on gold electrodes for detection of organophosphorus pesticides.[20] The aim of the present study is to design an amperometric biosensor for estimating the levels of putrescine in nanomolar concentrations. The introduction of the nano-interface in the present work is expected to improve the detection levels of putrescine in nanomolar ranges and exhibit fast response time below 5 seconds.

## 2. Materials and methods

### 2.1. Materials

Diamine oxidase from porcine kidney, diethyl carbodiimide and iron(II) chloride were purchased from M/s Sigma Aldrich Co, Ltd (India). Sodium dihydrogen phosphate, sodium potassium tartrate, disodium hydrogen phosphate, Folin–Ciocalteu's phenol reagent, iron(III) chloride and ascorbic acid were purchased from Merck (India). All chemicals were used as such without further purification and solutions were prepared using deionized water.

### 2.2. Synthesis of iron oxide nanoparticles

Iron oxide nanoparticles were synthesized by a thermal co-precipitation method. The thermal co-precipitation using ferric and ferrous chlorides was carried out according to the method reported by Kouassi *et al.*[21] Briefly, 0.25 M iron(II) chloride and iron(III) chloride were dissolved in double distilled water at a ratio of 1 : 2 and chemically precipitated at room temperature (25 °C) by adding ammonium hydroxide solution (30% v/v) at pH 10–10.4. The solution was heated at 80 °C for 35 minutes under continuous stirring. Impurities were removed from the iron oxide nanoparticles by centrifuging several times at 2800 rpm in water followed by ethanol. The iron oxide nanoparticles in the slurry form were then dried at 70 °C in a vacuum oven.

### 2.3. Linking of DAO to iron oxide nanoparticles

DAO was covalently linked to the iron oxide nanoparticles according to the method reported by Kouassi *et al.*[21] 50–70 mg of iron oxide nanoparticles were added to 1 mL of phosphate buffer saline solution (0.1 M, pH 7.2). After adding 0.5 mL of *N*-(3-dimethylaminopropyl)-*N*′-ethylcarbodiimide hydrochloride solution (0.02 g $mL^{-1}$ in phosphate buffer), the mixture was sonicated for 15 minutes for the carbodiimide activation, following which 10 μL of DAO (10 mg $mL^{-1}$) was added and further sonicated at 4 °C for 30 minutes. The mixture was centrifuged at 3000 rpm and the precipitate containing free and $Fe_3O_4$ bound DAO was washed with 0.1 M phosphate buffer (pH 7.2) followed by 0.1 M Tris–HCl buffer (pH 8.0) and with 0.1 M NaCl to enhance the separation of the iron oxide nanoparticles.

### 2.4. Determination of immobilization efficiency

The immobilization efficiency of the DAO enzyme onto the iron oxide nanoparticles was determined by the amount of free enzyme content in the supernatant which was estimated using Folin–Ciocalteu's phenol reagent by spectrophotometry at 660 nm. The following relation was used to calculate the percentage immobilization of the enzyme

$$\text{Immobilization}\% = \frac{\text{Total amount of enzyme added} - \text{free enzyme}}{\text{Total amount of enzyme added}} \times 100$$

Published on 21 October 2011 on http://pubs.rsc.org | doi:10.1039/C1AN15637C
Downloaded by University of Guelph on 07 September 2012

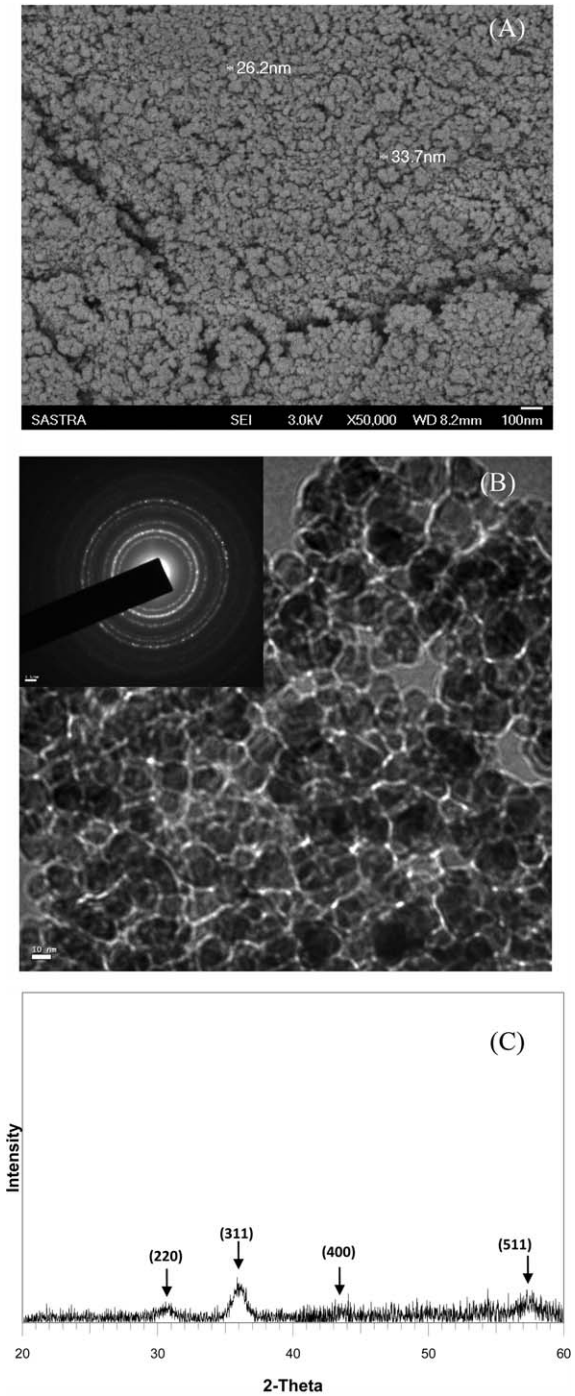


**Fig. 1** (A) Scanning electron micrograph of iron oxide nanoparticles; (B) transmission electron micrograph image of the iron oxide nanoparticles. Inset shows the *d*-spacing; (C) powder X-ray diffraction pattern of iron oxide nanoparticles.

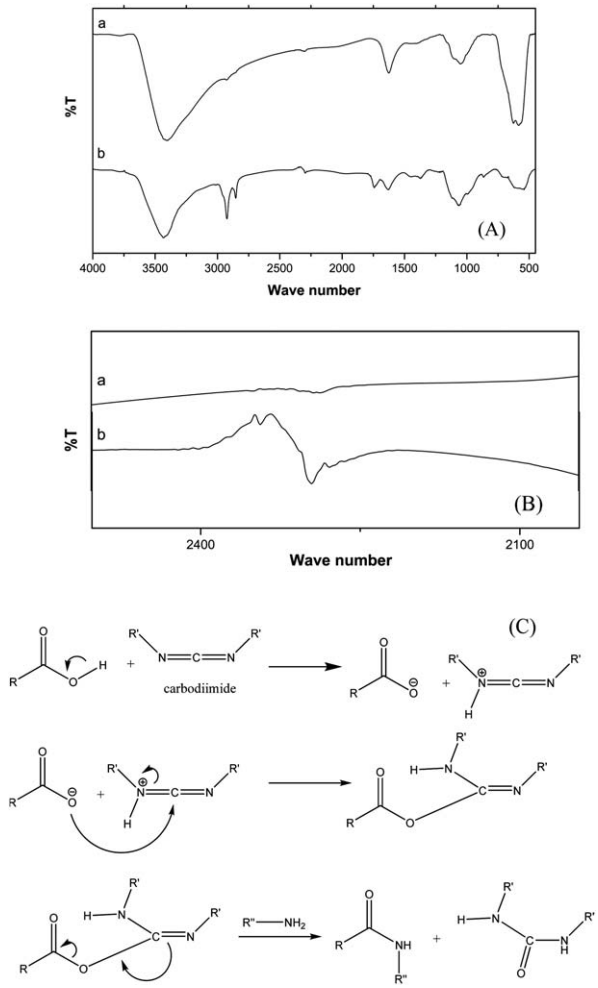


**Fig. 2** (A) FT-IR spectra (4000–400 $cm^{-1}$) of iron oxide nanoparticles (a) and DAO immobilized iron oxide nanoparticles (b). (B) FT-IR spectra between 2000 and 2500 $cm^{-1}$ of iron oxide nanoparticles (a) and DAO immobilized iron oxide nanoparticles (b). (C) Reaction mechanism showing the formation of the amide bond.

## 2.5. DAO tagged iron oxide nanoparticles coating onto the glassy carbon electrode

Glassy carbon (GC) electrode was subjected to cleaning by ultrasonication in acetone solution followed by de-ionized water for about 10 minutes in each medium. The enzyme tagged iron oxide nanoparticles were evenly coated with the help of a thin layer of carbon paste, which was spread on the GC electrode tip. The carbon paste acts as an embedding interface between the glassy carbon and the DAO tagged iron oxide nanoparticles.[13] Finally 5 μL of Nafion solution was added and air dried. Nafion acts as a protective coating for the enzyme tagged iron oxide nanoparticles. The modified electrode was then air dried for 2 hours and the electrode is referred to as DAO/nano-$Fe_3O_4$/GC.

## 2.6. Characterization techniques

**2.6.1. Iron oxide characterization.** The morphology of the iron oxide nanoparticles was studied using a cold field emission scanning electron microscope (FE-SEM) (JSM 6701F, JEOL, Japan) while the crystalline nature of the iron oxide nanoparticles was characterized by X-ray diffraction (XRD) (D8 Focus, Bruker, Germany) which was performed from an angle 10° to 60°. A field emission transmission electron microscope (FE-TEM) (JSM 2100, JEOL, Japan) was also used for the morphological and determination of *d*-spacing. The iron oxide

 This journal is © The Royal Society of Chemistry 2011

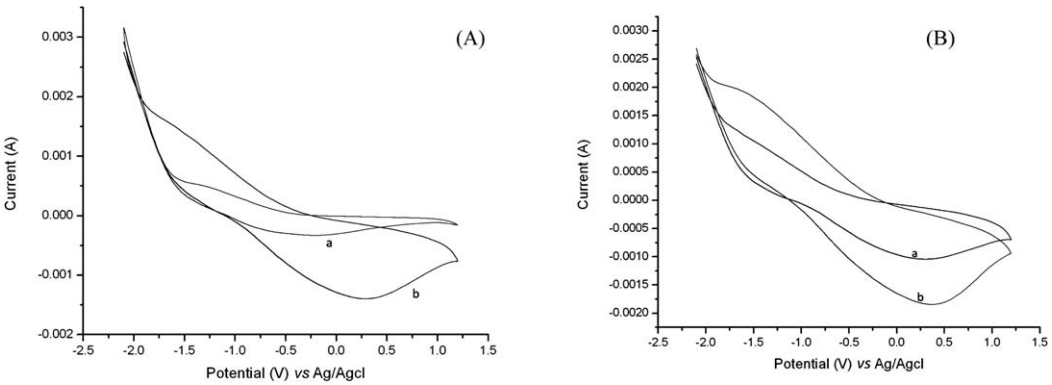


**Fig. 3** Control voltammograms: (A) cyclic voltammograms at a scan rate of 0.1 V $s^{-1}$ *vs.* Ag/AgCl in phosphate buffer of pH 7.2 in the absence of putrescine for (a) DAO/GC and (b) DAO/nano-$Fe_3O_4$/GC electrodes; (B) in the presence of putrescine for (a) DAO/GC and (b) DAO/nano-$Fe_3O_4$/GC electrodes.

Published on 21 October 2011 on http://pubs.rsc.org | doi:10.1039/C1AN15637C
Downloaded by University of Guelph on 07 September 2012

nanoparticles and the enzyme tagged iron oxide nanoparticles were analysed using Fourier transform infrared spectroscopy (FT-IR) (Spectrum 100, Perkin Elmer, USA). The spectrum was recorded at a resolution of 4 $cm^{-1}$ averaging 15 scans between 4000 and 400 $cm^{-1}$. The immobilization efficiency of the enzyme DAO was estimated by UV-visible spectrophotometry (Lambda 25, Perkin Elmer, USA) at 660 nm, using Lowry's method.

**2.6.2. Electrochemical analysis.** Electrochemical analysis was carried out with an electrochemical analyzer (CHI600C, CH Instruments, USA) with DAO/nano-$Fe_3O_4$/GC as a working electrode, Ag/AgCl as a reference electrode and platinum wire as a counter electrode. Cyclic voltammograms (CVs) were recorded at a scan rate of 0.1 V $s^{-1}$ in pH 7.2 phosphate buffer with DAO/nano-$Fe_3O_4$/GC at 25 °C. Owing to the low potential range and

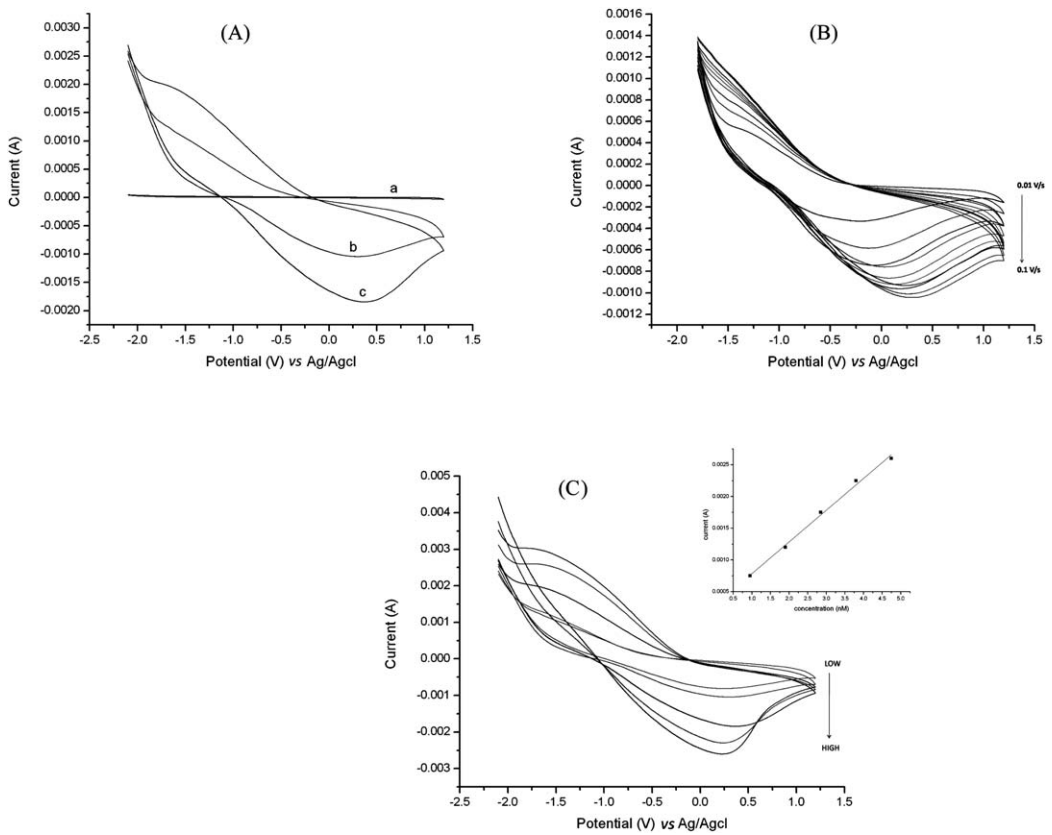


**Fig. 4** (A) Cyclic voltammograms at a scan rate of 0.1 V $s^{-1}$ *vs.* Ag/AgCl in phosphate buffer of pH 7.2 to show the effect of putrescine. (a) Bare glassy carbon electrode, (b) GC electrode coated with iron oxide, (c) GC electrode coated and modified with iron oxide and DAO enzyme. (B) Cyclic voltammograms for DAO/nano-$Fe_3O_4$/GC at various scan rates (0.01 V $s^{-1}$ to 0.1 V $s^{-1}$) in the presence of 0.95 nM putrescine. (C) Cyclic voltammograms for DAO/nano-$Fe_3O_4$/GC at various concentrations of putrescine (0.95 nM to 4.75 nM) at a scan rate of 0.1 V $s^{-1}$. Inset shows the calibration plot between concentration of putrescine and the corresponding current.

Published on 21 October 2011 on http://pubs.rsc.org | doi:10.1039/C1AN15637C
Downloaded by University of Guelph on 07 September 2012

good electrochemical inertness, the glassy carbon electrode was chosen for amperometric studies. The amperometric *i–t* curve was recorded for successive additions of putrescine to 5 mL of 0.1 M phosphate buffer (pH 7.2) at an applied potential of +0.4 V.

## 3. Results and discussion

### 3.1. Characterization of iron oxide nanoparticles

The surface morphology of the synthesized iron oxide nanoparticles observed with a field emission scanning electron microscope is shown in Fig. 1(A). Uniform spherical morphology of the nanoparticles was observed with a size ranging from 25–35 nm. The transmission electron micrographs reveal the *d*-spacing as 0.2 nm which is shown in Fig. 1(B). The powder X-ray diffraction pattern of the iron oxide nanoparticles is shown in Fig. 1(C). The pattern indicates the polycrystalline nature of the particles. The characteristic peaks at 30.17°, 36° and 57.23° in the $2\theta$ scale confirm the formation of $Fe_3O_4$. The peak positions are well in agreement with JCPDS (65-3107) and are indexed to (311), (400) and (511). The low intense broad peaks indicate the nanosize of the particles.

**FT-IR spectroscopy.** The FT-IR spectra of iron oxide nanoparticles and DAO immobilized iron oxide nanoparticles is shown in Fig. 2(A&B). Both the iron oxide and the enzyme tagged iron oxide exhibit the vibration band of Fe–O bond at 591 $cm^{-1}$. This shows the presence of iron oxide. DAO tagged iron oxide exhibits unique bands at 2390 $cm^{-1}$ and 1723 $cm^{-1}$ corresponding to –C–N– stretch and –C═O stretch which are absent in the pristine iron oxide spectrum. This confirms the presence of the enzyme in the modified iron oxide sample. The covalent linking is likely due to the formation of an amide bond (Fig. 2 (C)) resulting from the reaction between a carboxyl group on the enzyme and an amine group on the nanoparticle surface (specifically, the C–O to C–N conversion).[22]

**Determination of immobilization efficiency using a UV-visible spectrophotometer.** The immobilization efficiency is confirmed using the Folin–Ciocalteu reagent at a $\lambda_{max}$ of 660 nm. The experiments were carried out in triplicate and the immobilization efficiency of DAO was found to be 86–89%. The absorption maxima of the enzyme do not shift after sonication as in the case of free enzyme thus confirming that the immobilized enzyme does not denaturate.

### 3.2. Electrochemical studies with DAO/nano-$Fe_3O_4$/GC electrode

Control experiments were carried out using DAO/GC and DAO/nano-$Fe_3O_4$/GC electrodes, and the cyclic voltammograms in the absence and presence of putrescine analyte are shown in Fig. 3 (A) and (B). A slight increase in current is observed even in the presence of iron oxide alone. This may be attributed to the formation of $Fe_2O_3$ when it reacts with oxygen as $Fe_3O_4$ is susceptible to oxidation.[23] The cyclic voltammograms obtained at a scan rate of 0.1 V/s *vs.* Ag/AgCl are shown in Fig. 4(A). The voltammetry was carried out using phosphate buffer saline solution at pH 7.2. When comparing the overlayed plots, it can be seen that the bare glassy carbon electrode did not have any characteristic peak when 0.95 nM putrescine was added, while iron oxide modified electrode showed an increase in current on addition of same concentration of putrescine. However, it was observed that the voltammogram of diamine oxidase/iron oxide modified electrode had the highest current due to the catalytic reaction that occurs on the addition of putrescine, which is converted into hydrogen peroxide.

$$H_2N(CH_2)_4NH_2 + O_2 + H_2O \xrightarrow{DAO} H_2N(CH_2)_3CHO + NH_3 + H_2O_2$$

$$H_2O_2 \xrightarrow[+0.4\ V\ vs.\ Ag/AgCl]{GC} 2H^+ + O_2 + 2e^-$$

The effect of scan rate on the cyclic voltammogram for a DAO/nano-$Fe_3O_4$/GC electrode system is illustrated in Fig. 4(B), with different scan rates 0.01, 0.02, 0.03, 0.04, 0.05, 0.06, 0.07, 0.08, 0.09 and 0.1 V $s^{-1}$. The peak current increases linearly as the scan rate increases due to a progressive decrease in the diffusion layer near the electrode thereby causing an increase in the electron transfer rate and hence in the current. However, a marked shift in the peak is also observed with increasing scan rate, which indicates that the electron transfer is slower than the voltage scan rate which is a characteristic of the quasi-reversible or irreversible electrode reactions.[24] The CV curves show relatively oblique shape instead of the flat shapes, which may be due to the poor contact between the electrode materials and electrode surface and/or the poor conductivity of electrode materials.

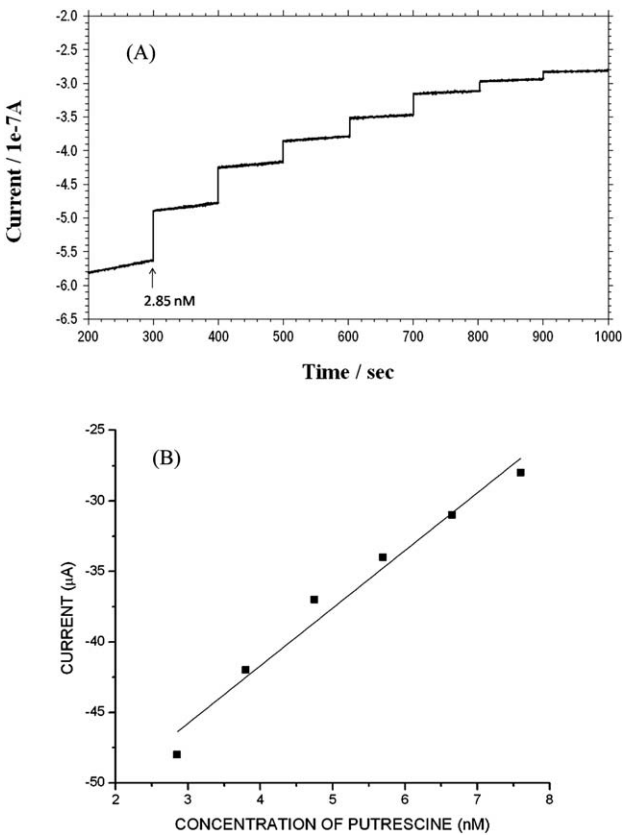


**Fig. 5** Amperometric *i–t* curve for a DAO/nano-$Fe_3O_4$/GC electrode. (A) Amperometric *i–t* curve showing stepwise increase in the current and (B) calibration plot for the linear range of concentrations of putrescine.


This journal is © The Royal Society of Chemistry 2011

Published on 21 October 2011 on http://pubs.rsc.org | doi:10.1039/C1AN15637C
Downloaded by University of Guelph on 07 September 2012

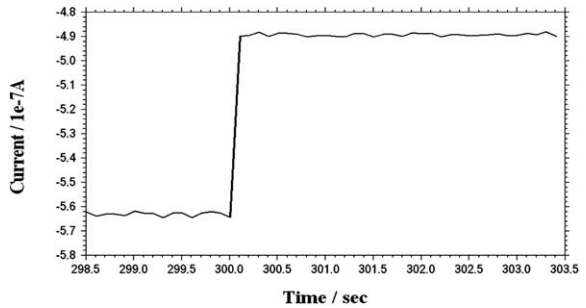


**Fig. 6** Response time illustration in amperometric *i–t* curve of a DAO/nano-$Fe_3O_4$/GC electrode.

The effect of increasing concentration of putrescine in the cyclic voltammogram for DAO/nano-$Fe_3O_4$/GC is illustrated in Fig. 4(C) showing a progressive increase in the current due to the production of hydrogen peroxide by the action of diamine oxidase on the putrescine in the analyte solution. The inset in the figure shows the linear relation between the putrescine concentration and the current.

Fig. 5 illustrates the amperometric pattern for increasing concentration of putrescine. The current measured for successive addition of 0.95 nM putrescine showed a step-wise increasing pattern in the current. The sharp increase in current is due to the enhanced electron transfer rate triggered by the nanointerface introduced in the glassy carbon electrode (Fig. 5(A)). The calibration plot is shown in Fig. 5(B).

As the concentration is increased by the addition of putrescine there was a steep increase in the current and consecutive additions lead to steep increasing steps with a response time of 0.3 seconds (Fig. 6). The iron oxide nanoparticles facilitate faster electron transfer from enzyme to the electrode and are responsible for very short response time. Similar short response time was reported by Fumio Mizutani *et al.* for monolayer enzyme modified glassy carbon electrodes.[25]

The specificity of the designed biosensor was monitored by the addition of ascorbic acid, since it is a well-known interfering agent in peroxide measurements as it oxidises at the same potential as $H_2O_2$. The current profile shown in Fig. 7, confirms that the diamine oxidase-based biosensor did not show any response on addition of ascorbic acid indicating high degree of specificity.

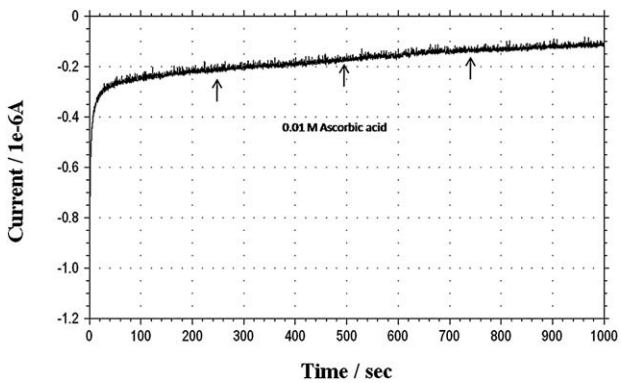


**Fig. 7** Effect of the interfering agent ascorbic acid in the amperometric *i–t* curve.

Thus, the overall sensing may be attributed to the presence of nanoparticles on the electrode surface which enhance the electron transfer rate thereby facilitating the oxidation of $H_2O_2$ at a lower voltage of +0.4 V instead of +1.2 V reported for unmodified glassy carbon electrodes.[26]

To check the stability of the developed sensor, continuous cyclic voltammetric measurements were carried out for 50 cycles. The peak current decreases by 4% after 10 cycles. The storage of the modified DAO/$Fe_3O_4$ NPs/GCE electrode was checked by immersing it in a phosphate buffer solution of pH 7.4 over a period of 2 weeks. The results demonstrate that the modified electrode exhibited a long storage time of 6 days after which the current reduced by 35% after the 7$^{th}$ day.

## 4. Conclusions

Iron oxide nanoparticles were synthesized and characterized using FE-SEM, FE-TEM, XRD, FT-IR and were modified with diamine oxidase enzyme. Characterization of the enzyme tagged iron oxide nanoparticles was carried out using FT-IR, which showed the presence of free and immobilized iron oxide. The electrochemical studies performed using a DAO/nano-$Fe_3O_4$/GC electrode showed a quasi-reversible pattern at the electrode. The DAO/nano-$Fe_3O_4$/GC electrode exhibited a linear response between 2 and 8 nM, with 0.65 nM as the minimal detection limit. The system possesses high selectivity and the response time was found to be 0.3 seconds and has the ability to detect very minimal concentration of the putrescine at a rapid time interval. The ultrafast detection of low amounts of putrescine can be used for clinical and analytical purposes.

## Acknowledgements

The authors are grateful to the Nano Mission Council, (No. SR/NM/PG–16/2007) Department of Science & Technology (DST), India for the financial support and to the Drugs & Pharmaceutical Research Programme, DST for providing the FE-TEM (VI-D&P/267/08-09/TDT). CH electrochemical analyzer was bought under the DST grant DST/TSG/PT/2008/28. We also thank SASTRA University, Thanjavur for the infrastructural support.

## Notes and references

1 P. H. M. Hoet, D. Dinsdale, C. P. L. Lewis, E. K. Verbeken, J. M. Lauweryns and B. Nemery, *Thorax*, 1993, **48**, 1235.
2 O. M. Rennert, W. Y. Chan, H. Hidalgo, W. Cushing and G. Griesmann, *Clin. Chim. Acta*, 1980, **103**, 375.
3 K. Sakata, K. Kashiwagi, S. Sharmin, S. Ueda, Y. Irie, N. Murotani and K. Igarashi, *Biochem. Biophys. Res. Commun.*, 2003, **305**, 143.
4 Y. Saeki, N. Uehara and S. Shirakawa, *J. Chromatogr., Biomed. Appl.*, 1978, **145**, 221.
5 J. Tamaoki, A. Chiyotani, E. Tagaya, K. Isono and K. Konno, *Mediators Inflammation*, 1994, **3**, 125.
6 D. F. Hwang, S. H. Chang, C. Y. Shiua and T. Chai, *J. Chromatogr., Biomed. Appl.*, 1997, **693**, 23.
7 C. X. Xu, S. A. M. Marzouk, V. V. Cosofret, C. R. P. Buck, M. R. Neuman and R. H. Sprinkle, *Talanta*, 1997, **44**, 1632.
8 L. Nagy, G. Nagy, R. E. Gyurcsányi, M. Neuman and E. Lindner, *J. Biochem. Biophys. Methods*, 2002, **53**, 165.
9 P. Bouvrette, K. B. Male, J. H. T. Luong and B. F. Gibbs, *Enzyme Microb. Technol.*, 1997, **20**, 32.
10 K. M. Kafi, D. Lee, S. Park and Y. Kwon, *J. Nanosci. Nanotechnol.*, 2007, **11**, 4005.

View Online

11 R. Gasparini, M. Scarpa, M. L. Paolo, R. Stevanato and A. Rigo, *J. Electroanal. Chem.*, 1991, **320**, 307.
12 J. Lange and C. Wittmann, *Anal. Bioanal. Chem.*, 2002, **372**, 276.
13 K. Thandavan, S. Gandhi, S. Sethuraman, J. B. B. Rayappan and U. M. Krishnan, *Nanotechnology*, 2011, **26**, 265505.
14 D. Sivalingam, J. B. Gopalakrishnan, U. M. Krishnan, S. Madanagurusamy and J. B. B. Rayappan, *Phys. E.*, 2011, **43**, 1804.
15 C. X. Guo, F. Hu, C. M. Li and P. K. Shen, *Biosens. Bioelectron.*, 2008, **24**, 819.
16 C. X. Guo, X. T. Zheng, Z. S. Lu, X. W. Lou and C. M. Li, *Adv. Mater.*, 2010, **22**, 5164.
17 C. X. Guo, Z. M. Sheng, Y. Q. Shen, Z. L. Dong and C. M. Li, *ACS Appl. Mater. Interfaces*, 2010, **2**, 2481.
18 C. X. Guo, X. T. Zheng, S. Ri Ng, Y. Lai, Y. Lei and C. M. Li, *Chem. Commun.*, 2011, **47**, 2652.
19 A. Kaushik, R. Khan, P. R. Solanki, P. Pandey, J. Alam, S. Ahmad and B. D. Malhotra, *Biosens. Bioelectron.*, 2008, **24**, 676.
20 N. Chauhan and C. S. Pundir, *Anal. Chim. Acta*, 2011, **701**, 66.
21 G. K. Kouassi, J. Irudayaraj and G. McCarty, *J. Nanobiotechnol.*, 2005, **3**, 1.
22 J. Jordan, C. S. S. R. Kumar and C. Theegala, *J. Mol. Catal. B: Enzym.*, 2011, **68**, 139.
23 L. Sophie, F. Delphine, P. Marc, R. Alain, R. Caroline, V. E. Luce and R. N. Muller, *Chem. Rev.*, 2008, **108**, 2064.
24 X. Wang, L. Wang and J. Wang, *J. Polym. Sci., Part B: Polym. Phys.*, 2004, **42**, 2245.
25 F. Mizutani, S. Yabuki, Y. Sato and Y. Hirata, *Polym. Sens.*, 1998, **690**, 46.
26 J. Z. Stemple, K. M. Rusin and T. L. Fare, *Anal. Chem.*, 1991, **63**, 1050.

Published on 21 October 2011 on http://pubs.rsc.org | doi:10.1039/C1AN15637C
Downloaded by University of Guelph on 07 September 2012

 This journal is © The Royal Society of Chemistry 2011